*Environmental Guardian*
https://www.sciltp.com/journals/eg

*Article*

# Valorization of Eggshell Waste: Extraction and Characterization of Calcium Carbonate

Neeraj Ravi * and Rakesh Kumar Soni

Department of Chemistry, Chaudhary Charan Singh University, Meerut 250004, India
* Correspondence: neerajravi9012@gmail.com

**How To Cite:** Ravi, N.; Soni, R.K. Valorization of Eggshell Waste: Extraction and Characterization of Calcium Carbonate. *Environmental Guardian* **2026**, *1*(1), 6.

Received: 14 July 2026
Revised: 15 September 2026
Accepted: 28 September 2026
Published: 18 November 2026

**Abstract:** Eggshell waste generated from households, bakeries, and food-processing industries is an abundant bio resource rich in calcium carbonate. This study investigates the recovery and characterization of highly pure calcium carbonate derived from discarded eggshells. The collected eggshells were washed, dried, pulverized and subjected to purification procedures to obtain $CaCO_3$. The resulting product was examined using a range of analytical techniques, including Fourier Transform Infrared Spectroscopy (FTIR), X-ray Diffraction (XRD), Transmission Electron Microscopy (TEM), Scanning Electron Microscopy coupled with Energy-Dispersive X-ray Spectroscopy (SEM–EDX) and particle-size analysis. FTIR spectra verified the formation of calcite-structured calcium carbonate through its characteristic vibrational bands. SEM observations indicated a porous crystalline surface, while EDX measurements identified calcium, carbon, and oxygen as the predominant elemental components. TEM images revealed mainly spherical and cube-shaped calcite nanoparticles with dimensions smaller than 10 nm. XRD patterns displayed the typical reflections of calcite, and the average crystallite size was estimated to be about 34.38 nm using the Debye–Scherrer formula. Particle-size measurements further confirmed the nanostructured characteristics of the synthesized material. The findings indicate that eggshell waste can serve as a sustainable and cost-effective source of nano-calcium carbonate with high purity and desirable physicochemical properties. The extracted $CaCO_3$ contributes to waste valorization, resource recovery, and environmental sustainability.

**Keywords:** eggshell waste; calcium carbonate; waste valorization; Nano-$CaCO_3$; characterization

## 1. Introduction

Knowing that marble, limestone, and chalk all began in shallow water, investigating calcium carbonate could reveal a great deal about the history of the planet. Calcium carbonate is colorless and odorless in powder form. It dissolves readily in acid, but it is only marginally soluble in water.

$CaCO_3$ is the chemical formula for the compound Calcium Carbonate. It is a common material present in rocks together with aragonite and calcite minerals. Furthermore, the main ingredient in pearls, snail shells, and the eggs of marine animals is calcium carbonate, which is extracted through mining or quarrying. However, calcium oxide can also be used to produce calcium carbonate. Initially calcium oxide is dissolved in water to form $Ca(OH)_2$. Then carbon dioxide is passed through the solution, resulting in the precipitation of calcium carbonate, as shown in Scheme 1 [1,2].

Precipitated calcium carbonate (PCC) and ground calcium carbonate (GCC) are the two main categories of calcium carbonate. PCC is perfect for manufacturing paper because of its extremely tiny and regulated particle size. GCC, on the other hand, is a powdered substance made from limestone that is extensively utilized in numerous

**Copyright:** © 2026 by the authors. This is an open access article under the terms and conditions of the Creative Commons Attribution (CC BY) license (https://creativecommons.org/licenses/by/4.0/).
**Publisher's Note**: Scilight stays neutral with regard to jurisdictional claims in published maps and institutional affiliations.

industrial and pharmacological applications [3]. Many of us first come into contact with calcium carbonate when we use chalkboards in the school. A fine, microcrystalline substance is chalk. The composition of egg shells is quite similar to that of human teeth and bones. The $CaCO_3$ content varied among the different types of eggshells, as shown in Table 1. Additionally, it promotes bone repair. It aids in the healing of bones as well. It is mostly employed in the polymer industry and other industrial settings. Many polymers employ $CaCO_3$ as a filler. Under typical conditions, hexagonal β-$CaCO_3$ or the crystal calcite, is the thermodynamically stable form of $CaCO_3$. The other forms are orthorhombic λ-$CaCO_3$, which occurs as the mineral aragonite and can form by precipitation at temperatures above 85 °C, and hexagonal λ-$CaCO_3$, which occurs as the mineral viterite and may form by precipitation around 60 °C [4].

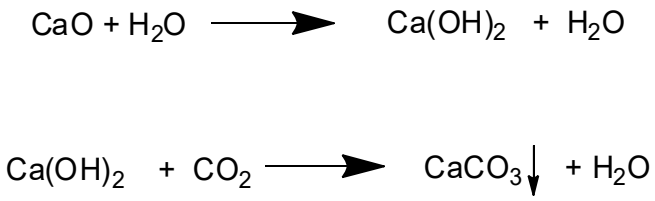

**Scheme 1.** Synthesis of $CaCO_3$.

The three minerals that are pure calcium carbonate are Vaterite, Calcite and Aragonite. Rocks that are mostly composed of calcium carbonate, such as chalk, marble, travertine and limestone [5,6], are key sources for industry [7]. The primary biological sources of calcium carbonate are Egg Shells, seashells and snail shells. These materials can also be exploited as industrial sources of the chemical. In addition to being a practical industrial resource, oyster shells have recently become more well-known as a dietary source of calcium [8,9].

In this study, calcium carbonate was isolated from egg shell waste and analyzed using a variety of analytical methods, including XRD (X-ray diffraction), SEM (scanning electron microscopy), TEM (transmission electron microscopy), and FTIR (Fourier Transform Infrared spectroscopy). Using weaker diffraction technique (Malvern equipment, Malvern, Worcestershire, UK), the particle size distribution was further examined. Figure 1 shows a diagrammatic representation of the present study.

**Table 1.** $CaCO_3$ content and weight in various bird egg shells [10].

| Weight of $CaCO_3$ in (gm) | The % of $CaCO_3$ in Egg Shell | Sample Eggs |
|---|---|---|
| 0.4764 | 95.28% | Hybrid hen |
| 0.4 | 80% | Local hen |
| 0.4344 | 87% | Domestic Pigeon |
| 0.4554 | 91% | Forest Pigeon |
| 0.3403 | 68.06% | Swift |
| 0.4823 | 96.46 | Lap wing |

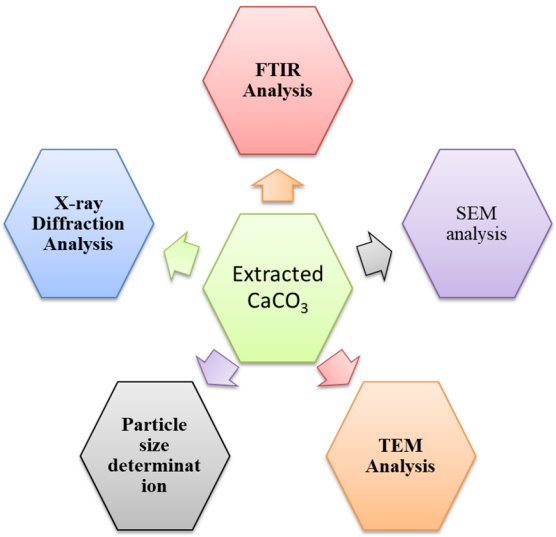


**Figure 1.** Diagrammatic representation of present chapter.

## 2. Experimental

### *2.1. Chemicals*

Waste egg shells were obtained from the nearby local bakery shops and restaurants and cleaned thoroughly by washing with acetic acid/soap water and then rinsed distilled water.

### *2.2. Method of Calcium Carbonate Extraction*

Calcium carbonate was extracted from egg shells using a number of precise steps, as shown in Figure 2.

#### 2.2.1. Collection and Pre Treatment

Approximately 100 g of egg shells were collected from food processing facilities, restaurants or households and thoroughly washed with distilled water to remove residual egg white, membranes, and other adhering organic matter. The cleaned eggshells were then treated with 5% (*v*/*v*) acetic acid solution at a solid-to-liquid ratio of 1:5 (g/mL) for 40 min at room temperature. Following acid treatment, the eggshells were washed three times with distilled water until the wash water reached approximately neutral pH.

#### 2.2.2. Drying

After cleaning, the egg shells were dried in a hot-air oven at 60 °C for 2 h to remove residual moisture. The dried eggshells were then allowed to cool to room temperature before grinding into powder for subsequent processing.

#### 2.2.3. Grinding

The dried egg shells were ground using a laboratory grinder to obtain a fine powder. The grinding process increased the specific surface area of the egg shell particles, facilitating subsequent processing and chemical treatment. The resulting powder was collected and used for further purification.

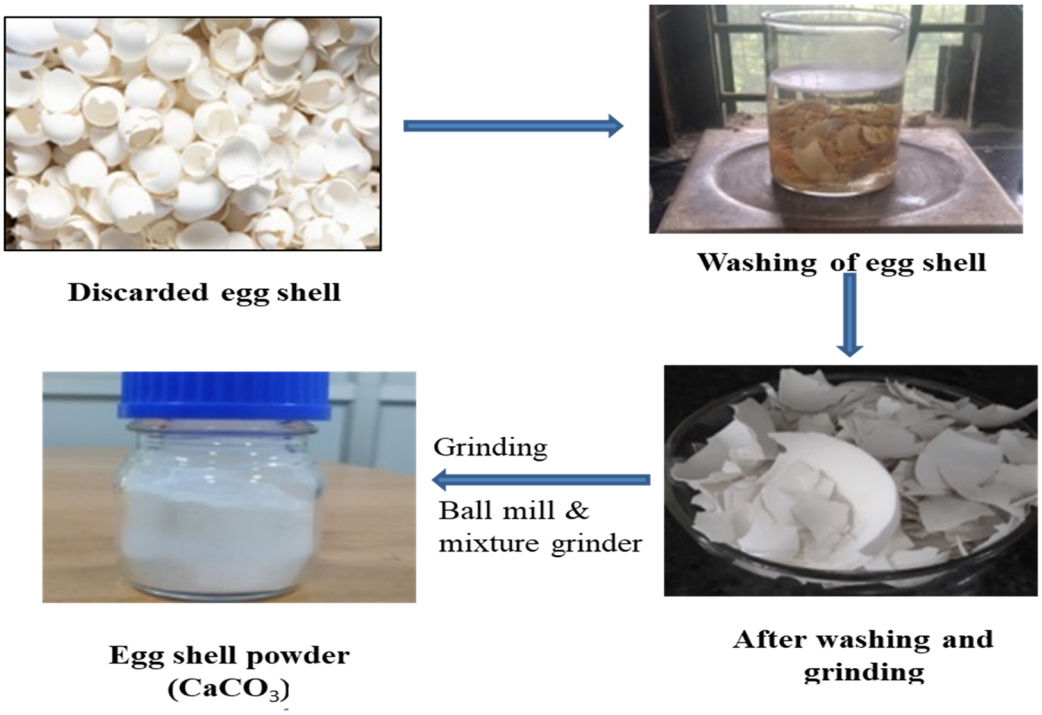


**Figure 2.** Flow diagram of extraction of Calcium Carbonate.

#### 2.2.4. Purification

The obtained egg shell-derived calcium carbonate was washed three times with distilled water to remove soluble impurities. After each washing cycle, the solid material was separated by filtration using Whatman No. 1 filter paper. The filtered material was then dried in a hot-air oven at 60 °C for 2 h to remove residual moisture. After drying, the material was cooled to room temperature and collected for further characterization.

## 3. Characterization of Extracted Calcium Carbonate

The ground Egg Shell powder was characterized using FTIR Spectroscopy, Scanning Electron Microscopy and X-ray diffraction, Transmission Electron Microscopy. Further investigation of the particle size distribution was performed using lesser diffraction technology (Malvern instrument).

The Rigakuminiflux 600 X-ray diffractometer operating in the reflection mode Cu-Ka radiation (40 kV, 15 mA) and diffracted beam monochromator was used for XRD measurements. A step scan mode with a step of 0° to 80° (2θ) was used. The Debye Scherrer formula was used to estimate the average crystallite size of $CaCO_3$ powder made from egg shell.

$$D = K\lambda/B\ Cos\theta \quad (1)$$

Here, D stands for average crystallite size in nm, K for dimensionless form factor (K = 0.9), λ for X-ray wavelength (k = 1.54056 A° for Cu Ka radiation), B for full breadth at half maximum, and θ for Bragg's diffraction angle (θ). The greatest intensity in the XRD pattern was used to calculate the size of $CaCO_3$ after the FWHM value was converted to radians (Equation (1).

## 4. Results and Discussions

### *4.1. FT-IR Study of Egg Shell Derived $CaCO_3$*

Figure 3 presents the overlaid FTIR spectra of eggshell-derived $CaCO_3$ (ES-$CaCO_3$) and commercially available $CaCO_3$ (C-$CaCO_3$). The characteristic absorption bands observed in the spectra are primarily associated with the vibrational modes of the $CO_3^{2-}$ group. The prominent band observed at approximately 1396 $cm^{-1}$ in ES-$CaCO_3$ can be assigned to the asymmetric C–O stretching vibration of the carbonate group [11]. The band near 870 $cm^{-1}$ is attributed to the out-of-plane bending vibration of $CO_3^{2-}$, while the band at 715 $cm^{-1}$ corresponds to the in-plane bending vibration [12–15]. These characteristic carbonate bands are consistent with the calcite polymorph of $CaCO_3$.

A weak band at 1084 $cm^{-1}$, corresponding to the symmetric stretching vibration of $CO_3^{2-}$, is characteristically observed for aragonite but is generally absent or very weak in calcite because of the symmetry dependent infrared selection rules. Therefore, the absence of a distinct band around 1084 $cm^{-1}$ in the ES-$CaCO_3$ spectrum is consistent with the calcite structure. In contrast, the additional band around 1084 $cm^{-1}$ observed in the commercial $CaCO_3$ spectrum, together with its associated carbonate vibrational features, suggests a contribution from the aragonite polymorph. The FTIR spectrum of ES-$CaCO_3$ therefore exhibits the characteristic vibrational pattern expected for calcite, with no distinct aragonite-associated band near 1084 $cm^{-1}$. The similarity of the major carbonate bands between the two samples supports the presence of $CaCO_3$, whereas the differences in the positions and presence of the polymorph sensitive bands provide evidence for differences in crystalline phase. The absence of additional bands associated with organic functional groups further indicates effective removal of the eggshell membrane and other organic components during the extraction process [16].

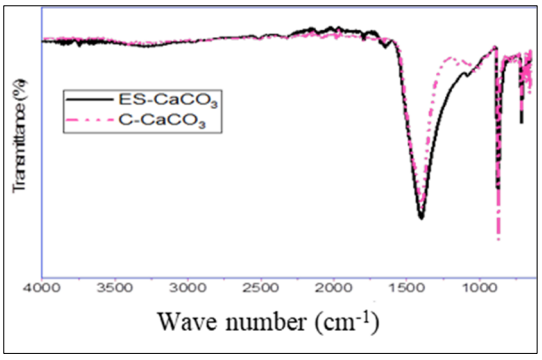


**Figure 3.** Overlayed Spectra of Commercial $CaCO_3$ (C-$CaCO_3$) and derived from Egg shell derived $CaCO_3$ (ES-$CaCO_3$).

### *4.2. SEM Analysis with EDX Spectra*

Figure 4 shows an SEM micrograph of egg shell derived $CaCO_3$ at a magnification of 58.88 KX, along with the corresponding EDX spectra. Table 2 lists the weight and atomic percentages of the relevant elements. SEM photomicrographs of calcite calcium carbonate extracted from egg shell waste reveal that the powder is predominantly crystalline and porous.

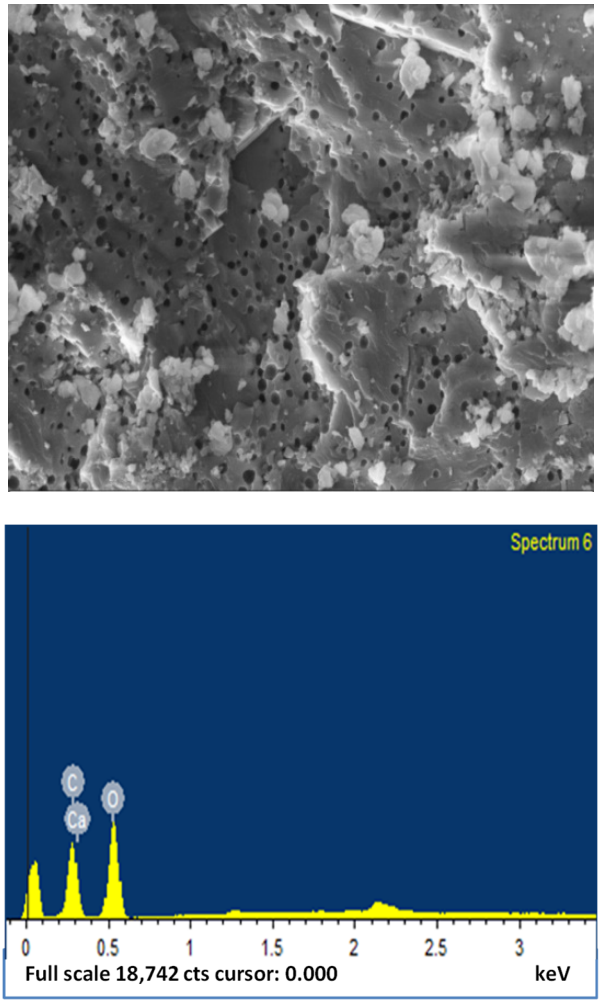


**Figure 4.** SEM micrograph of Egg Shell derived $CaCO_3$ with EDX spectrum.

Compared to raw calcitic rock in the given literature, the synthesized $CaCO_3$ nanomaterial exhibits a different morphology [17].

The EDX analysis showed Ca, C, and O contents of 28.17, 20.38, and 51.46 wt%, respectively. The corresponding atomic percentages were 12.51, 30.21, and 57.28 at% for Ca, C, and O, respectively. These values differ from the theoretical composition of stoichiometric $CaCO_3$ (40.04 wt% Ca, 12.00 wt% C, and 47.96 wt% O), with a lower apparent Ca content and relatively higher apparent C and O contents. Such deviation was observed due to the semi-quantitative nature of SEM–EDX analysis, particularly for light elements, owing to contributions from the carbon tape used for sample mounting. In powder samples, the electron-beam interaction volume extends beyond the $CaCO_3$ particles into the underlying carbon tape or surrounding material, resulting in an enhanced carbon signal and consequently a reduced normalized Ca percentage. Previous studies have reported that carbon detected during EDX analysis can originate from carbon-based mounting substrates. Furthermore, variations in particle size, morphology, surface roughness, measurement location, interaction volume, and matrix effects influenced the measured elemental composition [18]. Therefore, the EDX values should be regarded as representative of the analyzed region rather than as an exact representation of the bulk stoichiometric composition of $CaCO_3$. The slight deviation in the total weight percentage (100.01%) from 100% is attributable to rounding of the individual elemental percentages.

**Table 2.** The corresponding elements' weight and atomic percentages in the extracted calcium carbonate.

| Component | Experimental | |
|---|---|---|
| | Weight Percent (%) | Atomic Percent (%) |
| C K | 20.38 | 30.21 |
| O K | 51.46 | 57.28 |
| Ca K | 28.17 | 12.51 |
| Total | 100.01 | 100.00 |

*4.3. Transmission Electron Microscopy Analysis*

TEM photographs of the extracted $CaCO_3$ are shown in Figure 5, revealing predominantly spherical particles with relatively smooth surfaces. The TEM analysis indicated that the observed primary particles were predominantly below 10 nm, confirming their nanoscale dimensions. In addition, some nanosized cubic-like structures were observed, which were consistent with the characteristic morphology commonly associated with calcite $CaCO_3$. However, the observed morphology was considered supportive rather than definitive for phase identification, which was established through complementary characterization. The nanoscale particle morphology suggested a high surface-area-to-volume ratio, which could contribute to enhanced surface reactivity and make the extracted $CaCO_3$ potentially suitable for applications in nanocomposites, advanced coatings, pharmaceuticals, and other high-performance materials. Overall, the TEM observations had provided important information regarding the morphology and primary particle dimensions of the extracted $CaCO_3$.

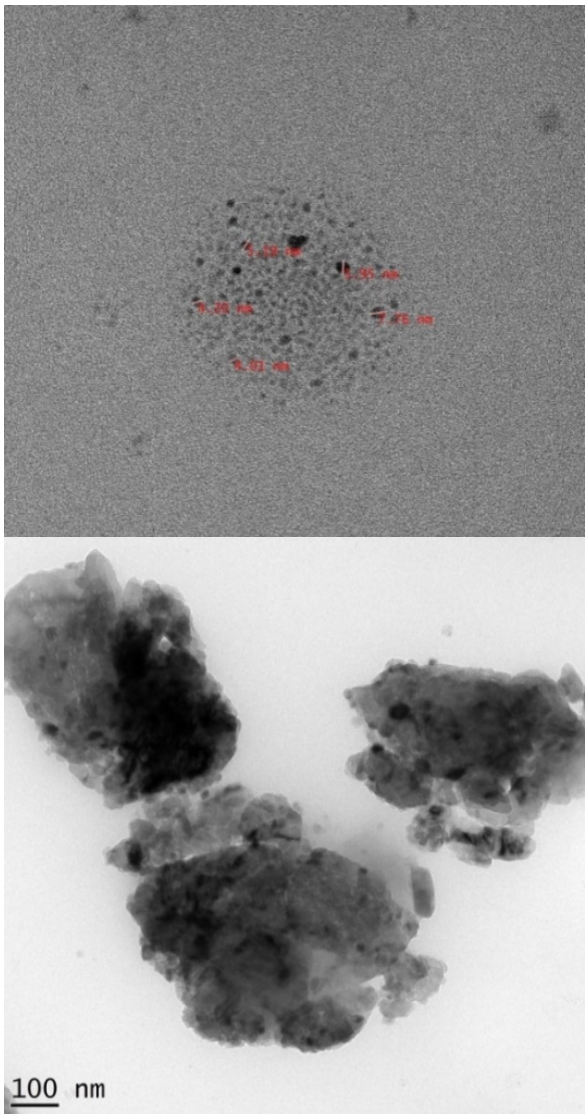


**Figure 5:** TEM micrograph of Egg Shell derived $CaCO_3$.

*4.4. Particle Size Determination*

The PSD was conducted using particle size distribution theory, indicates that the particle sizes of the extracted $CaCO_3$ range from approximately 1 to 1.586 nanometers (nm) as shown in Figure 6. This broad range highlights the variability in particle sizes within the sample. The distribution is expressed in terms of volume percentage; therefore, the observed maximum of approximately 30% represents the volume contribution around this particle-size region rather than the percentage of individual particles. Notably, the analysis revealed that around 30% of the particles have a diameter of approximately 1.586 nanometers, placing them firmly in the nanoscale range. The presence of such a significant proportion of nanoscale particles is indicative of the fine and homogeneous nature of the extracted $CaCO_3$.

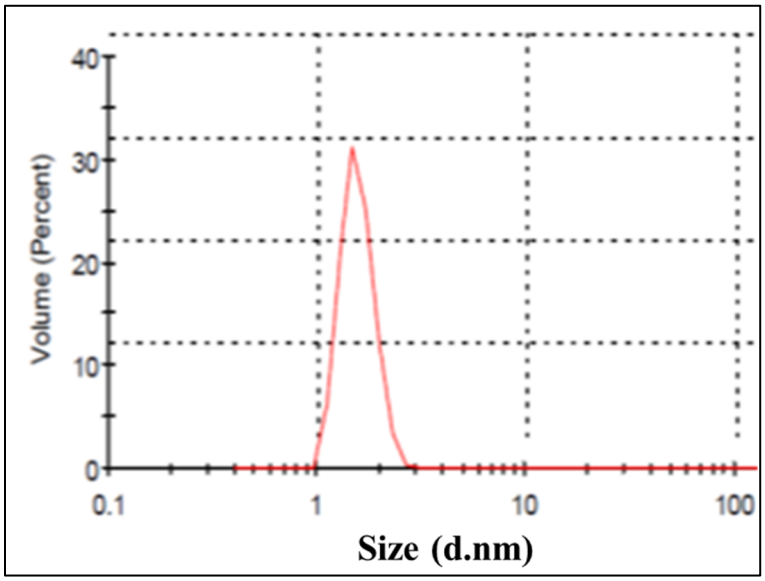


**Figure 6.** Particle Size Distribution of Egg Shell derived $CaCO_3$.

The nano scale size of these particles is particularly relevant for various applications, including pharmaceuticals, high performance materials and advanced coatings. Nanometer sized particles offer enhanced surface area to volume ratios, which can lead to improved reactivity and functionality compared to larger particles. This fine particle size also supports the effective use of $CaCO_3$ in applications demanding exactcontrol over particle dimensions, like as in nano composites or as additives in specialty products [18,19].

*4.5. Analysis of X-ray Diffraction*

The crystalline nature of $CaCO_3$ obtained from eggshells was examined using powder X-ray diffraction (PXRD). Figure 7 shows the PXRD pattern of the eggshell-derived $CaCO_3$. The diffraction pattern exhibits characteristic reflections of the calcite phase, with the most intense reflection observed at $2\theta = 29.34°$ [20]. The other experimentally observed calcite reflections are listed in Table 3, along with their corresponding crystallographic planes and previously reported values. The observed peak at 29.34° is in close agreement with previously reported calcite $CaCO_3$ values of approximately 29.4–29.5°. Previous XRD studies have reported characteristic calcite reflections in this region, consistent with the characteristic diffraction pattern of calcite. The close agreement between the experimental and reported diffraction peaks supports the identification of the extracted $CaCO_3$ as predominantly calcite.

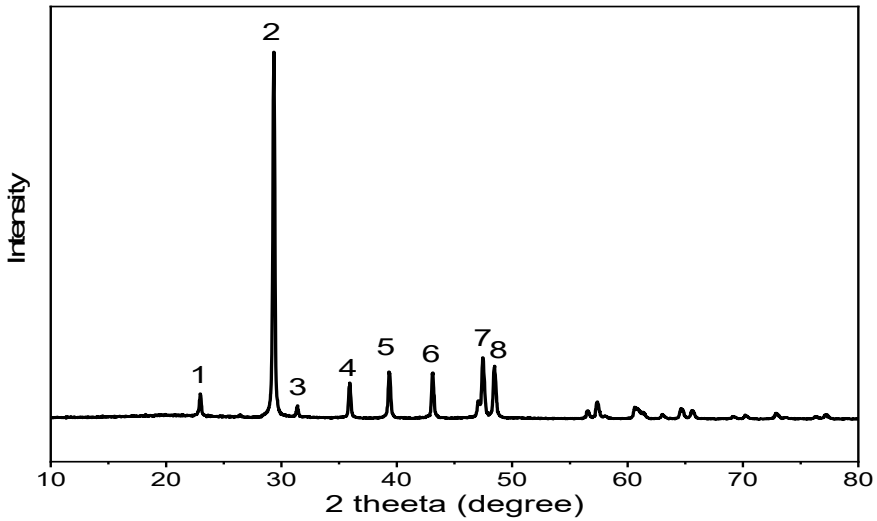


**Figure 7.** PXRD pattern of Egg shell derived $CaCO_3$.

The observed diffraction peaks are consistent with the standard diffraction pattern of calcite $CaCO_3$, indicating that the extracted material predominantly possesses a calcite crystalline structure. The crystallite size

was estimated using the Debye–Scherrer equation (Equation (1)), based on the FWHM values obtained from the diffraction peaks using Origin software. The FWHM values were converted into radians and used in the Scherrer equation, and the calculated average crystallite size was 34.38 nm (Table 3). The crystallite size estimated using the Scherrer equation represents the size of the coherent crystalline domains and does not directly correspond to the physical particle size [21–23]. The crystallite size may differ from the particle size because an individual particle can consist of one or more crystalline domains. In addition, peak broadening may be influenced by instrumental broadening and microstrain, which can affect the estimated crystallite size. Accordingly, the XRD-derived value of 34.38 nm is considered the average crystallite size of the $CaCO_3$ sample and should not be interpreted as a direct measure of its physical particle size.

**Table 3.** Sample's peak at relative intensity at 100 percent.

| No. | Peak Position [$^0$2Θ] | FWHM | Size of Crystallite D (nm) | D Average (nm) |
|---|---|---|---|---|
| 1. | 22.96 | 0.2381 | 34.04 | 34.38 |
| 2. | 29.34 | 0.2117 | 38.79 | |
| 3. | 31.37 | 0.2169 | 38.03 | |
| 4. | 35.91 | 0.2286 | 36.52 | |
| 5. | 39.36 | 0.2473 | 34.11 | |
| 6. | 43.11 | 0.2334 | 36.59 | |
| 7. | 47.47 | 0.3225 | 26.90 | |
| 8. | 48.47 | 0.2894 | 30.10 | |

## 5. Conclusions

In this chapter, calcium carbonate ($CaCO_3$) was successfully extracted from cost effective egg shell waste, resulting in high purity $CaCO_3$ with small crystallite sizes averaging 34.38 nanometers. The particle size distribution analysis revealed that 30% of the particles had a diameter of 1.586 nanometers, highlighting the nano scale nature of the material. Comprehensive characterization of the extracted $CaCO_3$ was performed using Fourier-transform Infrared Spectroscopy, Transmission Electron Microscopy and Scanning Electron Microscopy and X-ray Diffraction techniques. A particle size analyzer also offered comprehensive information on the distribution of particle sizes. SEM photomicrographs demonstrated that the $CaCO_3$ powder was predominantly crystalline with a porous structure, while TEM analysis showed particle diameters ranging between 1.5 and 10 nanometers. In future perspectives, $CaCO_3$ can be explored for advanced applications in biomedical materials, inorganic filler for PVC, environmental remediation, drug delivery and sustainable nanocomposites. Its low cost, abundance, biocompatibility, and tunable morphology make it a promising material for developing eco-friendly and high-performance functional materials.

## Author Contributions

N.R.: Writing—original draft, methodology, preparation of figures and tables; conceptualization, visualized the study, writing—reviewing and editing, investigated the study,; R.K.S.: supervision, conceptualization validation. All authors have read and agreed to the published version of the manuscript.

## Funding

This research received no external funding.

## Institutional Review Board Statement

Not applicable.

## Informed Consent Statement

Not applicable.

## Data Availability Statement

Data will be made available on request.

## Conflicts of Interest

Given the role as Journal Editor, Prof. Rakesh Kumar Soni had no involvement in the peer review of this paper and had no access to information regarding its peer-review process. Full responsibility for the editorial process of this paper was delegated to another editor of the journal."

## Use of AI and AI-Assisted Technologies

No AI tools were utilized for this paper.

## References


1. Kolekar, M.S.; Deshmukh, M.S.; Hiwale, M.V.; et al. Analyzation of calcium carbonate ($CaCO_3$) in eggshells and their applications. *Int. Res. J. Innov. Eng. Technol.* **2020**, *4*, 37–46. https://doi.org/10.47001/irjiet/2020.408007.
2. Hincke, M.T.; Nys, Y.; Gautron, J.; et al. The eggshell: Structure, composition and mineralization. *Front. Biosci.* **2012**, *17*, 1266. https://doi.org/10.2741/3985.
3. Cordeiro, C.M.M.; Hincke, M.T. Quantitative proteomics analysis of eggshell membrane proteins during chick embryonic development. *J. Proteom.* **2016**, *130*, 11–25. https://doi.org/10.1016/j.jprot.2015.08.014.
4. Wilson, P.B. Recent advances in avian egg science: A review. *Poult. Sci.* **2017**, *96*, 3747–3754. https://doi.org/10.3382/ps/pex187.
5. Sanders, D. Syndepositional dissolution of calcium carbonate in neritic carbonate environments: Geological recognition, processes, potential significance. *J. Afr. Earth Sci.* **2003**, *36*, 99–134. https://doi.org/10.1016/s0899-5362(03)00027-7.
6. Morse, J.W.; Arvidson, R.S.; Lüttge, A. Calcium carbonate formation and dissolution. *Chem. Rev.* **2007**, *107*, 342–381. https://doi.org/10.1021/cr050358j.
7. Hincke, M.T.; Da Silva, M.; Guyot, N.; et al. Dynamics of structural barriers and innate immune components during incubation of the avian egg: Critical interplay between autonomous embryonic development and maternal anticipation. *J. innate Immun.* **2019**, *11*, 111–124. https://doi.org/10.1159/000493719.
8. Halgrain, M.; Bernardet, N.; Crepeau, M.; et al. Eggshell decalcification and skeletal mineralization during chicken embryonic development: Defining candidate genes in the chorioallantoic membrane. *Poult. Sci.* **2022**, *101*, 101622. https://doi.org/10.1016/j.psj.2021.101622.
9. Athanasiadou, D.; Jiang, W.; Goldbaum, D.; et al. Nanostructure, osteopontin, and mechanical properties of calcitic avian eggshell. *Sci. Adv.* **2018**, *4*, eaar3219. https://doi.org/10.1126/sciadv.aar3219.
10. Sutapun, W.; Pakdeechote, P.; Suppakarn, N.; et al. Application of Calcined Eggshell Powder as Functional Filler for High Density Polyethylene. *Polym.-Plast. Technol. Eng.* **2013**, *52*, 1025–1033. https://doi.org/10.1080/03602559.2013.769578.
11. Szeleszczuk, Ł.; Pisklak, D.M.; Kuras, M.J.; et al. In VitroDissolution of Calcium Carbonate from the Chicken Eggshell: A Study of Calcium Bioavailability. *Int. J. Food Prop.* **2015**, *18*, 2791–2799. https://doi.org/10.1080/10942912.2015.1004587.
12. Galván-Ruiz, M.; Hernández, J.; Baños, L.; et al. Characterization of calcium carbonate, calcium oxide, and calcium hydroxide as starting point to the improvement of lime for their use in construction. *J. Mater. Civ. Eng.* **2009**, *21*, 694–698. https://doi.org/10.1061/(asce)0899-1561(2009)21:11(694).
13. Murugan, S.; Munusamy, Y.; Ismail, H. Effects of chicken eggshell filler size on the processing, mechanical and thermal properties of PVC matrix composite. *Plast. Rubber Compos.* **2017**, *46*, 42–51. https://doi.org/10.1080/14658011.2016.1260217.
14. Elfina, S.; Jamarun, N.; Arief, S.; et al. Sintesis Precipitate Calsium Carbonat Sebagai Filler Pada Plastik Ramah Lingkungan. *React. J. Res. Chem. Eng.* **2020**, *1*, 1. https://doi.org/10.52759/reactor.v1i1.4.
15. Murakami, F.S.; Rodrigues, P.O.; Campos, C.M.T.D.; et al. Physicochemical study of $CaCO_3$ from egg shells. *Ciência e Tecnol. de Aliment.* **2007**, *27*, 658–662. https://doi.org/10.1590/s0101-20612007000300035.
16. Saini, S.; Dhayal, V.; Leel, N.S.; et al. Reinforcing the characteristics of recyclable PVA/PVDF polymer blends via ZnO nanofiller. *Opt. Quantum Electron.* **2024**, *56*, 1943. https://doi.org/10.1007/s11082-024-07816-3.
17. Gora, M.K.; Kumar, A.; Choudhary, B.L.; et al. Electronic, structural and optical properties of Gd-doped ZnO powder synthesized by solid-state reaction method. *Bangladesh J. Sci. Ind. Res.* **2023**, *58*, 53–64. https://doi.org/10.3329/bjsir.v58i1.63634.
18. Ali, M.; Lin, F.; Tan, Y.; et al. Synthesis of micro-micro titanium composite powder with the electrostatic adsorption process. *Int. J. Adv. Manuf. Technol.* **2025**, *136*, 3215–3237. https://doi.org/10.1007/s00170-025-15003-1.
19. Holá, M.; Ondráček, J.; Bahelková, M.; et al. Characterization of laser-generated aerosols for ICP-MS: Experimental insights into particle size distribution, morphology, and composition. *Appl. Spectrosc. Rev.* **2026**, *61*, 495–536. https://doi.org/10.1080/05704928.2025.2567692.

20. Brodowski, S.; Amelung, W.; Haumaier, L.; et al. Morphological and chemical properties of black carbon in physical soil fractions as revealed by scanning electron microscopy and energy-dispersive X-ray spectroscopy. *Geoderma* **2005**, *128*, 116–129. https://doi.org/10.1016/j.geoderma.2004.12.019.
21. Lal, G.; Punia, K.; Dolia, S.N.; et al. Structural, cation distribution, optical and magnetic properties of quaternary $Co_{0.4}$ + $xZn_{0.6}$ − $xFe_2O_4$ (x= 0.0, 0.1 and 0.2) and Li doped quinary $Co_{0.4}$ + $xZn_{0.5}$ − $xLi_{0.1}Fe_2O_4$ (x= 0.0, 0.05 and 0.1) nanoferrites. *J. Alloys Compd.* **2020**, *828*, 154388. https://doi.org/10.1016/j.jallcom.2020.154388.
22. Palsaniya, K.K.; Kumari, N.; Dolia, S.N.; et al. Tailoring quantum dots through citric acid modulation of $CoFe_2O_4$ ferrite. *Mater. Chem. Phys.* **2024**, *313*, 128820. https://doi.org/10.1016/j.matchemphys.2023.128820.
23. Jakhar, N.; Alvi, P.A.; Choudhary, B.L. Exploring superparamagnetic behavior in MnxCo1-$xFe_2O_4$ quantum dots: A structural and spectroscopic investigation. *Inorg. Chem. Commun.* **2025**, *174*, 114058. https://doi.org/10.1016/j.inoche.2025.114058.